NANO LETTERS

2008
Vol. 8, No. 7
1813-1818

Ferroelectricity in Highly Ordered Arrays of Ultra-Thin-Walled $Pb(Zr,Ti)O_3$ Nanotubes Composed of Nanometer-Sized Perovskite Crystallites

Jongok Kim,[†] Sun A Yang,[†] Yong Chan Choi,[†] Jin Kyu Han,[†] Keum Ok Jeong,[†] Yong Ju Yun,[‡] Dong Jik Kim,[§] Sang Mo Yang,[§] Doohee Yoon,[||] Hyeonsik Cheong,[||] Ki-Seog Chang,[⊥] Tae Won Noh,[§] and Sang Don Bu*[,†]

Department of Physics, Chonbuk National University, Jeonju 561-756, Korea, Division of Advanced Technology, Korea Research Institute of Standards and Science, Daejeon 305-600, Korea, FPRD & ReCOE, Department of Physics and Astronomy, Seoul National University, Seoul 151-747, Korea, Department of Physics, Sogang University, Seoul 121-742, Korea, and Department of Chemistry, Korea Air Force Academy, Cheongwon 363-849, Korea

Received January 24, 2008; Revised Manuscript Received April 8, 2008

ABSTRACT

We report the first unambiguous ferroelectric properties of ultra-thin-walled $Pb(Zr,Ti)O_3$ (PZT) nanotube arrays, each with 5 nm thick walls and outer diameters of 50 nm. Ferroelectric switching behavior with well-saturated hysteresis loops is observed in these ferroelectric PZT nanotubes with P_r and E_c values of about 1.5 μC cm^{-2} and 86 kV cm^{-1}, respectively, for a maximum applied electric field of 400 kV cm^{-1}. These PZT nanotube arrays (10^{12} nanotubes cm^{-2}) might provide a competitive approach toward the development of three-dimensional capacitors for the terabyte ferroelectric random access memory.

Ferroelectric nanotubes are of great interest because of their peculiar physical properties on the nanoscale[1–3] and their wide range of potential applications.[4–9] Well-registered arrays of ferroelectric $Pb(Zr,Ti)O_3$ nanotubes (PZT-NTs) with concentric cylindrical electrodes could function as three-dimensional (3D) device elements in miniaturized ferroelectric random access memory (FRAM).[4–7] Because of the outstanding piezoelectric properties of PZT, PZT-NTs should have applications in fluidic delivery[8,9] and nanoelectromechanical systems.[4] PZT-NTs are among the most researched ferroelectric nanotubes because of their industrial importance. Luo et al. first demonstrated the successful fabrication of PZT microtubes with a wall thickness of tens of nanometers using the template wetting method.[5,6] Bharadwaja et al. outlined a process for optimizing the phase purity of the crystalline structure of PZT microtubes by preventing the reaction between PZT and the porous silicon template.[10] Alexe et al. reported the fabrication of PZT-NTs with a minimum inner diameter of 100 nm by using a positive template that enables the control of the wall thickness of the PZT-NTs.[11] The synthesis and characterization of PZT-NTs with a diameter of around 50 nm have not previously been reported and were achieved in our study.

In this Letter, we report the first instance of unambiguous ferroelectric properties of PZT-NT arrays with 5 nm thick walls and an outer diameter of 50 nm. Field emission transmission electron microscopy (FETEM) was used to show that these PZT-NTs are composed of perovskite nanocrystallites that form a tubular rolled-up grain network. The well-saturated, artifact-free hysteresis loops of the PZT-NTs are indicative of their ferroelectric switching behavior. The use of the pore arrays of porous alumina membranes (PAMs) facilitates the fabrication of tailored PZT-NT arrays with various diameters and wall thicknesses, as well as of complicated structures such as branched or stepped pores (Supporting Information, S1).

Highly ordered PZT-NT arrays were prepared using a template-directed method that integrates a sol−gel process with a spin-coating technique (Figure 1a; Supporting Information S2).[12,13] Unlike other template-directed methods,[10,14,15] no film is observed on the surface view field emission scanning electron microscopy (FESEM) images of the spin-

* Corresponding author: phone, +82-63-270-4264; fax, +82-63-270-3320; e-mail, sbu@chonbuk.ac.kr.
[†] Chonbuk National University.
[‡] Korea Research Institute of Standards and Science.
[§] Seoul National University.
[||] Sogang University.
[⊥] Korea Air Force Academy.

10.1021/nl080240t CCC: $40.75
Published on Web 06/10/2008

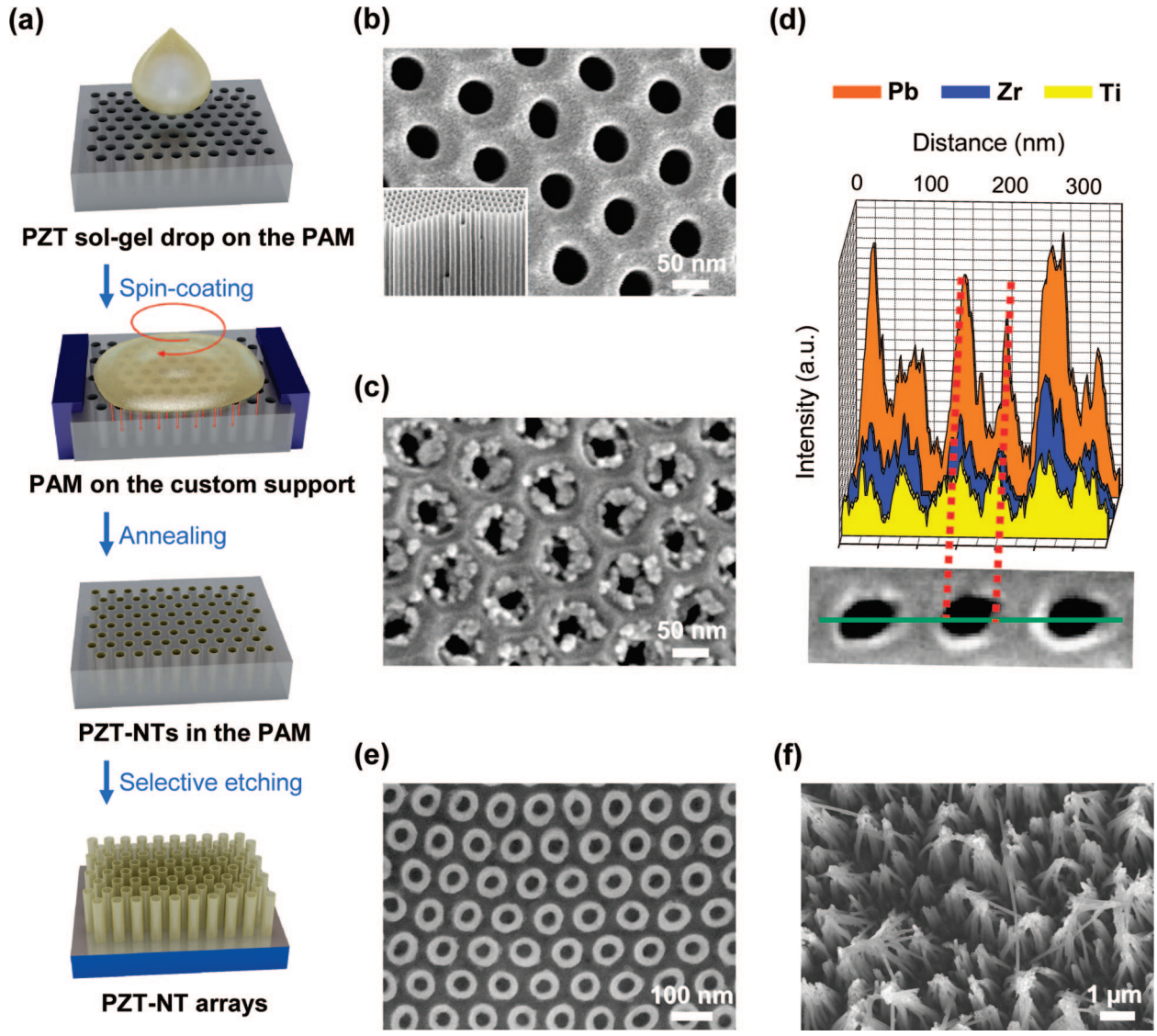

Figure 1. (a) A schematic illustration of the PZT-NT arrays synthesis procedure. (b) A surface view FESEM image of a typical PAM with a corresponding cross-sectional image shown in the inset. (c) A surface view FESEM image of a PAM after spin-coating with a PZT sol−gel solution. Note that the PZT-NTs are densely packed inside the PAM pores. (d) The lower part of this figure is a STEM image and the upper part is the EDS line profile along the green line in the STEM image. The dotted red line highlights the periodic intensity of Pb, Zr, and Ti in the sectioned PZT-NTs. (e) A FESEM image of a highly ordered hexagonal array of low aspect ratio (length/diameter ~6) PZT-NTs after wet chemical etching for 15 min with aqueous NaOH solution. (f) A FESEM image of high aspect ratio (~200) PZT-NTs etched for 30 min, resulting in their aggregation.

coated PAM (Figure 1b,c). The presence of a surface film causes several problems in the preparation of complicated structures such as metal/ferroelectric/metal concentric cylindrical capacitors, because it must be removed after the deposition of each layer by using either wet or dry etching. In our method, however, spin-coating not only assists the sols to enter the pores but also removes excess sols from the top surface. These results suggest that our method could be used to fabricate tailored PZT-NTs with precise control over wall thickness.

Scanning transmission electron microscopy (STEM) and energy dispersive X-ray spectroscopy (EDS) were performed on sectioned PZT-NTs to determine their chemical composition (Figure 1d). The STEM image (the lower part of Figure 1d) shows that there is bright contrast at the edges of the pores, which suggests that the tubes are comprised of heavier elements than Al and O, the main components of the PAM. The corresponding EDS scan (the upper part of Figure 1d) along the green line in the STEM image shows recurrent increases and decreases in the Pb, Zr, and Ti intensities along the sectioned PZT-NTs, indicating their periodicity. Thus, the contrast variation at the edges of the pores is due to their presence.

Once the host PAM is selectively dissolved, the PZT-NTs collapse into nanotube bundles (Figure 1f) because of the loss of mechanical support from the alumina and capillary force induced during a postgrowth cleaning process.[16,17] Microtubes with thicker walls would form arrays because of their low aspect ratios (<50).[4–6,8,10] However, our high aspect ratio (~200) PZT-NTs possess ultrathin walls (~5 nm; see Figure 4b) and so are unable to tolerate the capillary stress and thus lean against one another. One way to prepare

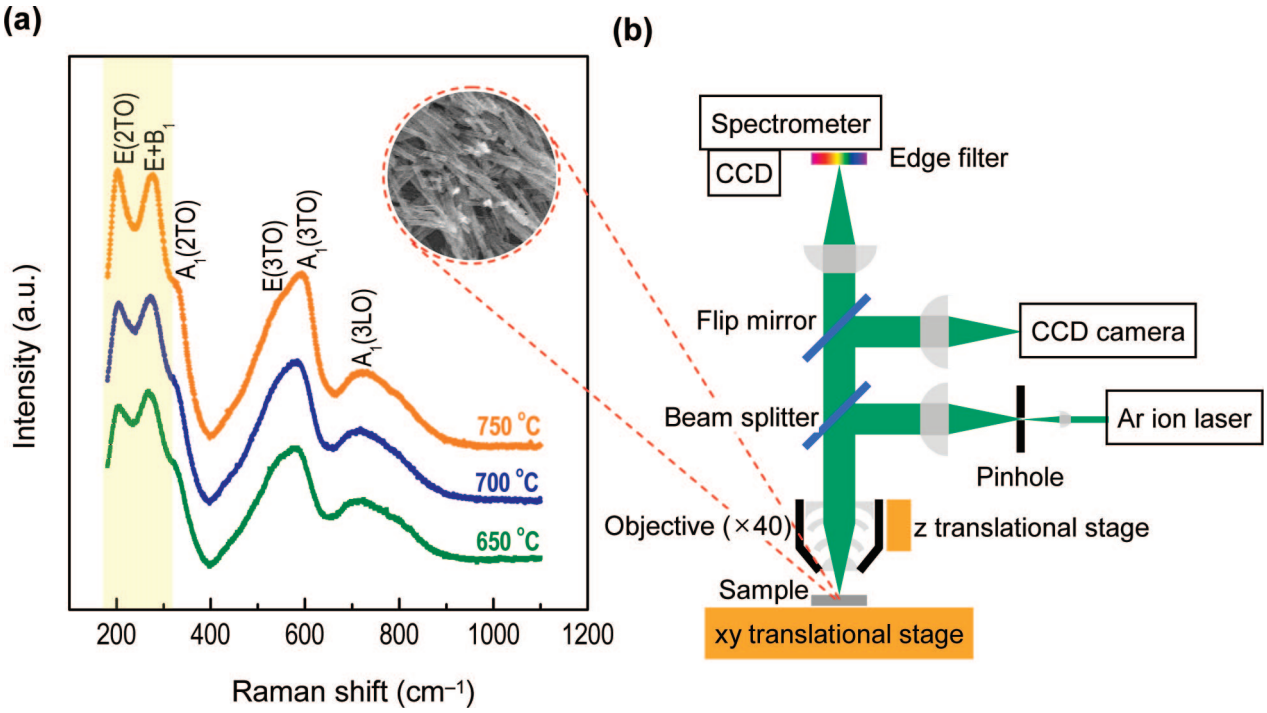

Figure 2. (a) Raman spectra of the PZT-NTs for various annealing temperatures. The spectra were obtained at room temperature with the 514.5 nm line of an Ar ion laser (~1.8 mW) focused on a 1 μm diameter spot (Nikon ×40, Numerical Aperture 0.6). The Raman peaks at wavenumbers 205, 275, 317, 533, 593, and 724 cm^{-1} are due to the E(2TO), E + B_1, A_1(2TO), E(3TO), A_1(3TO), and A_1(3LO) modes, respectively, of tetragonal PZT. In order to take into account changes in the intensity and peak sharpness with the variation in the annealing temperature, the spectra were normalized to the peak intensity of the A_1(2TO) mode. The Raman spectrum of the sample annealed at 750 °C has stronger and sharper Raman peaks than that of the sample annealed at 650 °C, which indicates improved crystallization as the temperature increases. The inset shows a representative FESEM image of the PZT-NTs collected on a stainless steel substrate. (b) Schematic diagram of the Raman spectroscopy setup.

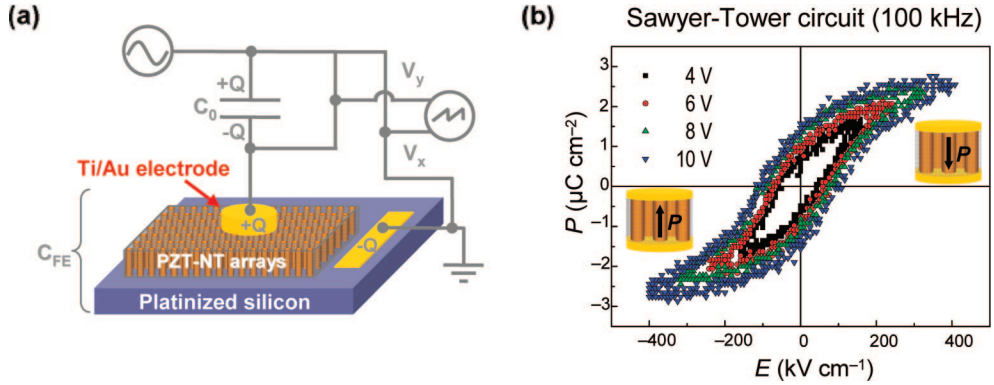

Figure 3. (a) A schematic diagram of the Sawyer−Tower circuit used to minimize the contribution of leakage current to the P−E hysteresis measurements. (b) Unambiguous P−E hysteresis loops obtained at 100 kHz with a Sawyer−Tower circuit with applied voltages between 4 and 10 V. The measured P_r and E_c are about 1.5 μC cm^{-2} and 86 kV cm^{-1} respectively.

arrays of ultra-thin-walled PZT-NTs is to reduce the aspect ratio by using a thin PAM (Supporting Information, S3). We prepared a perfect hexagonal array of PZT-NTs with an aspect ratio of 5, a diameter of 60 nm, and a length of 300 nm (Figure 1e). The long-range order of the arrays of PZT-NTs (Supporting Information, S3) shows that the array is an exact replica of the PAM, which highlights one of the most versatile aspects of the template-directed method: the shape and geometry of the arrays can be readily manipulated by varying the host template (Supporting Information S1,3).

Micro-Raman spectroscopy provides a very sensitive method for detecting tetragonal symmetry in nanoscale perovskite particles such as $BaTiO_3$[18,19] and was used to determine the phase of the PZT-NTs. Tetragonal PZT belongs to the space group $P4mm$, so $3A_1 + B_1 + 4E$ modes are observed in its Raman spectrum. Raman peaks (Figure 2a) are present at wavenumbers 205, 275, 317, 533, 593, and 724 cm^{-1}, identified as due to the E(2TO), E(silent) + B_1, A_1(2TO), E(3TO), A_1(3TO), and A_1(3LO) modes of PZT, respectively. The phonon modes of the PZT-NTs are typical of those found in the Raman spectra of perovskite PZT,[20] confirming the tetragonality of the prepared PZT-NTs. The increase in the intensity of the region of the spectrum highlighted in yellow (Figure 2a) clearly shows that the

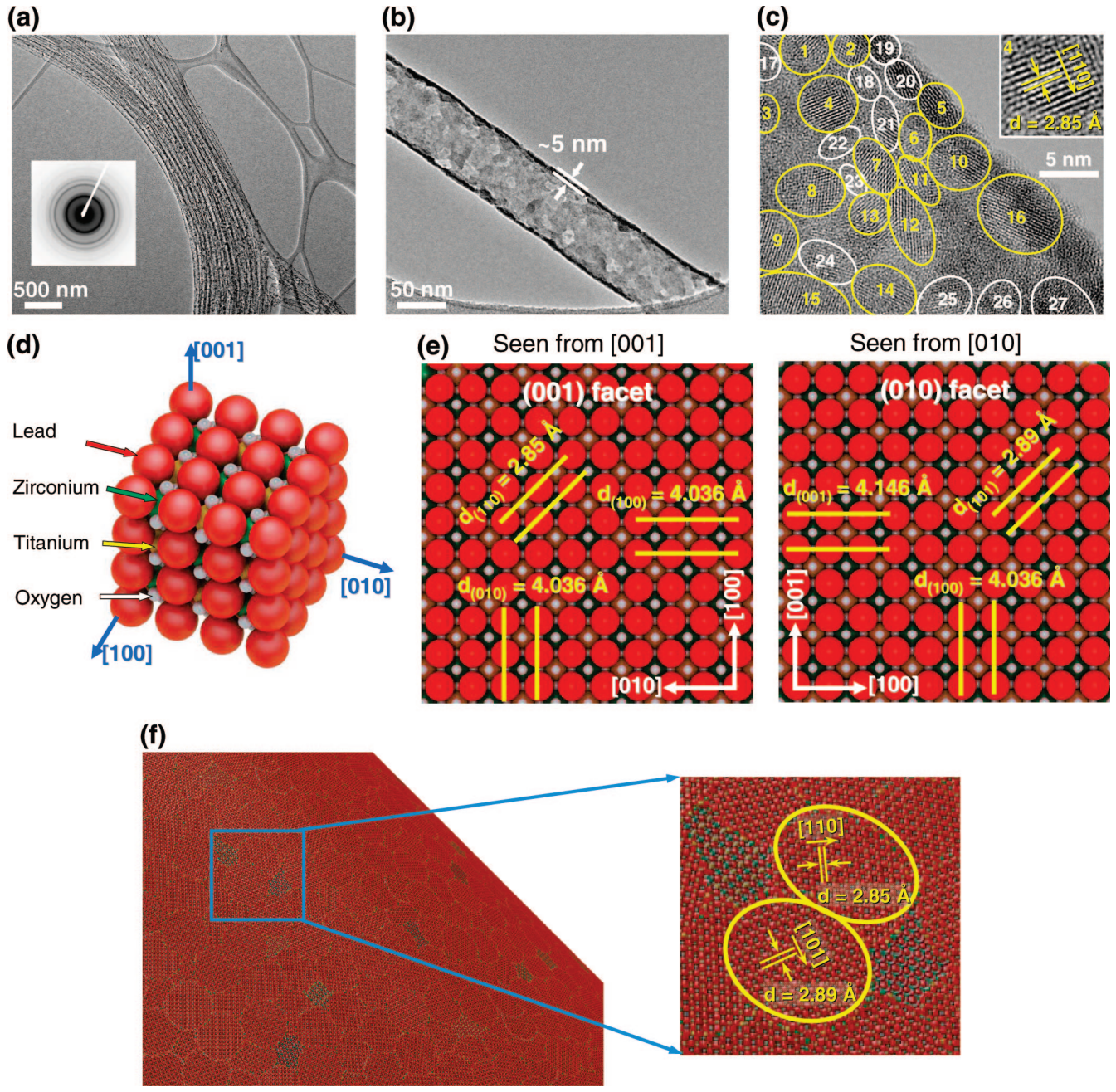

Figure 4. (a) A FETEM image of a bundle of high aspect ratio PZT-NTs, with its corresponding SAED ring pattern. (b) An individual PZT-NT with a wall thickness of approximately 5 nm. (c) A high-resolution image of a PZT-NT with perovskite grains of only a few nanometers in size, indicated by yellow circles and ellipses, which mostly have lattice spacings of 2.85 and 2.89 Å and are assigned to the (110) and (101) planes, respectively, of the tetragonal perovskite phase. Oxygen-deficient pyrochlore ($Pb_2Ti_2O_6$) and lead-deficient pyrochlore phases ($PbTi_3O_7$) can also be found, marked with white ellipses. (d) A 3D atomic representation of PZT nanocrystallites for only a few unit cells. The red, green, yellow, and white spheres represent lead, zirconium, titanium, and oxygen atoms, respectively. (e) Surface view atomic representations of the two most probable facets of PZT nanocrystallites with PbO termination: the representations on the left and right are seen from the [001] and [010] directions, respectively. (f) A schematic model of an ultra-thin-walled PZT-NT consisting of perovskite grains of only a few nanometers in size with the facets shown in Figure 4e.

crystallinity of the PZT-NTs improves with increases in the annealing temperature.

To check whether our PZT-NTs are ferroelectric, we determined the polarization−electric field ($P-E$) characteristic curves of metal/PZT-NTs/metal capacitors (see Figure 3a). The ferroelectric $P-E$ hysteresis loop (Supporting Information S4, in black) and displacement currents (Supporting Information S4, in red) were simultaneously recorded at 2 kHz with a TF analyzer. Although the hysteresis loop is elliptical due to the large leakage current, displacement current peaks (the blue asterisks in Supporting Information S4) are also present, implying the presence of spontaneous polarization (P_s) switching.

Since artifacts due to dielectric loss are apt to be highly frequency dependent,[9,21] we varied the measuring frequency to minimize the leakage current contribution. The frequency

was increased to 100 kHz, and the $P-E$ hysteresis loops were recorded with a Sawyer−Tower circuit and a digital oscilloscope (Figure 3a). As a result, distinct ferroelectric hysteresis loops were obtained for the ultra-thin-walled PZT-NTs with driving voltages of 4, 6, 8, and 10 V (Figure 3b). The increases in the coercive field (E_c) and the remanent polarization (P_r) with the driving voltage confirm that the PZT-NTs exhibit significant ferroelectric properties.

The PZT-NT capacitors exhibit well-saturated hysteresis loops with P_r and E_c values of about 1.5 μC cm^{-2} and 86 kV cm^{-1}, respectively, for a maximum applied electric field of 400 kV cm^{-1}. In order to take into account the geometrical dependence of P_r, the effective contact area of the capacitor was calculated and found to be ∼9% with respect to that of a PZT thin-film capacitor. The normalized P_r was thus estimated to be 17 μC cm^{-2}. These values for P_r and E_c are surprisingly similar to those of sol−gel derived polycrystalline PZT films,[22] despite the differences in geometry and the expected grain size induced effects.[15] These values cannot however be directly compared to those of bulk and thin films, since the measurements were performed with a nanotube-embedded PAM geometry that has a relatively intricate field distribution.[6]

We investigated the PZT-NTs with FETEM to determine their structural characteristics. The typical FETEM image of a free-standing PZT-NT bundle in Figure 4a shows its high aspect ratio. The appearance of selected area electron diffraction (SAED) rings (inset of Figure 4a) indicates that the nanotubes are polycrystalline. According to the electron diffraction formula, the major diffraction rings correspond to the (001), (110), (101), (111), (002), (102), and (112) reflections of the tetragonal phase of PZT, which were indexed by comparing the relative ratios of the d spacings with those deduced from JCPDS No. 33-0784. The high-resolution FETEM image in Figure 4c shows that the tube wall is composed of nanocrystallites with diameters in the range 3−7 nm (see Supporting Information S5). The striking similarity (compare Figure 4b and Figure 4c) in wall thickness and the size of the crystallites in the wall suggests that our ultra-thin-walled PZT-NTs form a tubular rolled-up grain network sheet consisting of perovskite PZT nanocrystallites (see Figure 4f).

These findings are consistent with recent reports of perovskite nanocrystallites with sizes of about 5 nm in ultrathin PZT nanorings[23] and of 2−3 nm in $PbTiO_3$ nanotubes.[14] In particular, these perovskite crystallites of just a few nanometers in size might only be found in ultra-thin-walled nanotubes or nanorings. PZT nanowires synthesized in a similar manner[13] also appear to consist of a mixture of perovskite and pyrochlore phases, but the nanometer-sized crystallites observed in the nanowires were determined to be of pyrochlore phase (Supporting Information S6). Such differences may be attributed to the combined effects of the annealing procedure,[24] the size effect from the nanotube dimensions,[14] and the host template,[15] which limit crystallite growth during the phase transition from pyrochlore to perovskite.

By comparing the lattice fringes and the SAED rings (see Supporting Information S5), we found that our PZT-NTs are a mixture of perovskite, lead-deficient pyrochlore phase ($PbTi_3O_7$), and oxygen-deficient pyrochlore phase ($Pb_2Ti_2O_6$). However, they primarily exhibit perovskite phase with a d spacing of 2.85 Å (110) (see the insets in Figure 4c,f), as evident in the high-resolution FETEM analysis (see Figure 4c and Supporting Information S5). Assuming these crystallites having the PbO surface termination,[25,26] the majority of PZT-NTs surfaces are determined to have either (010) and (001) facets and the surface atomic representations of these facets are reconstructed in Figure 4e. In order to determine the relative amounts of perovskite and pyrochlore phases in the nanotubes, we roughly calculated the volume ratio of perovskite (110) with respect to the sum of perovskite (110) and pyrochlore (222). The ratio of the perovskite phase in our PZT-NTs was estimated to be about 90%, which indicates their high quality. On the basis of this evidence, we suggest that the ultra-thin-walled PZT-NTs can be regarded as a rolled-up grain network sheet in a tubular form composed of nanosized perovskite crystallites (Figure 4f).

With their unambiguous ferroelectricity, the ultra-thin-walled PZT-NT arrays (10^{12} nanotubes cm^{-2}) reported here may represent a competitive approach toward the development of 3D capacitors for the terabyte FRAM[27] compared to the existing approaches.[28,29] These vertical arrays of PZT-NTs can be readily manipulated and so will facilitate the fabrication of more complicated structures for use in nanoelectromechanical systems. Moreover, these nanometer-sized perovskite grains also offer a promising material for the investigation of toroidal ordering in ferroelectrics.

Acknowledgment. This work was supported by the Korea Research Foundation of the Korean Government (MOEHRD) through Grant No. KRF-2005-005-J07501. We thank Ju Jin Kim, Byoung Kye Kim, and Eun Kyoung Jeon (Chonbuk National University, Korea) for their help with the electrical measurements and our fruitful discussions.

Supporting Information Available: Images showing varied pore arrays of PAMs and PZT nanowires and description of experimental methods This material is available free of charge via the Internet at http://pubs.acs.org.

References

(1) Naumov, I. I.; Bellaiche, L.; Fu, H. *Nature* **2004**, *432*, 737.
(2) Sheinerman, A. G.; Gutkin, M.; Yu, *Phys. Status Solidi A* **2001**, *184*, 485.
(3) Zhang, Q. M.; Wang, H.; Cross, L. E. *J. Mater. Sci.* **1993**, *28*, 3962.
(4) Alexe, M.; Luo, Y.; Szafraniak, I.; Wehrspohn, R. B.; Steinhart, M. A nanotube based cantilever arm, a method of operating and manufacturing a nanotube based cantilever arm, and a storage device and a photonic crystal based on an array of nanotube based cantilever arms. European Patent EP1439546A1, July 11, 2004.
(5) Luo, Y.; Szafraniak, I.; Nagarajan, V.; Wehrspohn, R. B.; Steinhart, M.; Wendorff, J. H.; Zakharov, N. D.; Ramesh, R.; Alexe, M. *Integr. Ferroelectr.* **2003**, *59*, 1513.
(6) Luo, Y.; Szafraniak, I.; Zakharov, N. D.; Nagarajan, V.; Steinhart, M.; Wehrspohn, R. B.; Wendorff, J. H.; Ramesh, R.; Alexe, M. *Appl. Phys. Lett.* **2003**, *83*, 440.
(7) Scott, J. F. *Ferroelectrics* **2005**, *314*, 207.
(8) Morrison, F. D.; Scott, J. F. *Processes of forming small diameter rods and tubes.* UK Patent GB2414246B, November 23, 2005.
(9) Scott, J. F. *Science* **2007**, *315*, 954.

(10) Bharadwaja, S. S. N.; Olszta, M.; Trolier-McKinstry, S.; Li, X.; Mayer, T. S.; Roozeboom, F. *J. Am. Ceram. Soc.* **2006**, *89*, 2695.
(11) Alexe, M.; Hesse, D.; Schmidt, V.; Senz, S.; Fan, H. J.; Zacharias, M.; Gösele, U. *Appl. Phys. Lett.* **2006**, *89*, 172907.
(12) Kim, J.; Choi, Y. C.; Bu, S. D. *Ferroelectrics* **2007**, *356*, 236.
(13) Choi, Y. C.; Kim, J.; Bu, S. D. *Mater. Sci. Eng., B* **2006**, *133*, 245.
(14) Zhao, L.; Steinhart, M.; Yu, J.; Gösele, U. *J. Mater. Res.* **2006**, *21*, 685.
(15) Hernandez-Sanchez, B. A.; Chang, K.-S.; Scancella, M. T.; Burris, J. L.; Kohli, S.; Fisher, E. R.; Dorhout, P. K. *Chem. Mater.* **2005**, *17*, 5909.
(16) Tanaka, T.; Morigami, M.; Atoda, N. *Jpn. J. Appl. Phys., Part 1* **1993**, *32*, 6059.
(17) Ahu, K.; Vinzant, T. B.; Neale, N. R.; Frank, A. J. *Nano Lett.* **2007**, *7*, 3739.
(18) Asiaie, R.; Zhu, W.; Akbar, S. A.; Dutta, P. K. *Chem. Mater.* **1996**, *8*, 226–234, 1996.
(19) Frey, M. H.; Payne, D. A. *Phys. Rev. B* **1996**, *54*, 3158.
(20) Burns, G.; Scott, B. A. *Phys. Rev. Lett.* **1970**, *25*, 1191.
(21) Dawber, M.; Rabe, K. M.; Scott, J. F. *Rev. Mod. Phys.* **2005**, *77*, 1083.
(22) Hoffmann, M.; Küppers, H.; Schneller, T.; Böttger, U.; Schnakenberg, U.; Mokwa, W.; Waser, R. *IEEE Trans. Ultrason. Ferroelectr. Freq. Control* **2003**, *50*, 1240.
(23) Zhu, X. H.; Evans, P. R.; Byrne, D.; Schilling, A.; Douglas, C.; Pollard, R. J.; Bowman, R. M.; Gregg, J. M.; Morrison, F. D.; Scott, J. F. *Appl. Phys. Lett.* **2006**, *89*, 122913.
(24) Schwartz, R. W. *Chem. Mater.* **1997**, *9*, 2325.
(25) Meyer, B.; Padilla, J.; Vanderbilt, D. *Faraday Discuss.* **1999**, *114*, 395.
(26) Jiang, B.; Peng, J. L.; Bursill, L. A.; Zhong, W. L. *J. Appl. Phys.* **2000**, *87*, 3462.
(27) In the realization of the practical terabyte FRAM, one important challenge for researchers and the industry is the so-called "cross-talk problem", which causes ferroelectric polarization of adjacent ferroelectric capacitors (FCs) other than the target FCs with respect to each FC when a reading or writing is performed. In the case of the PZT nanotubes presented in this letter, such a problem can be overcome by manipulating the host template geometry (e.g. Ken-ichi, I.; Hideki, M. *IEICE Tech. Rep*. **2007**, *106*, 29; *Fujitsu* **2007**, *58*, 90).
(28) Evans, P. R.; Zhu, X. H.; Baxter, P.; McMillen, M.; McPhillips, J.; Morrison, F. D.; Scott, J. F.; Pollard, R. J.; Bowman, R. M.; Gregg, J. M. *Nano Lett.* **2007**, *7*, 1134.
(29) Sun, C.-L.; Lam, K. H.; Chao, C.; Lau, S. T.; Chan, H. L. W.; Guo, S.; Zhao, X. *Appl. Phys. Lett.* **2007**, *90*, 253107.

NL080240T